

## Research on Road Crack Detection Based on Image Processing

Zhi Cui<sup>1</sup>, Yixiang Wang<sup>2</sup>

<sup>1</sup>College of Information and Electronic Engineering, Hunan City University, Yiyang, China

<sup>2</sup>College of Information and Electronic Engineering, Hunan City University, Yiyang, China

Corresponding Author: Zhi Cui

### ABSTRACT

Cracks are one of common road defects. Road crack detection is important for traffic safety. Image processing methods of road crack detection were studied. Through the comparison of average filtering, median filtering, and Wiener filtering, Wiener filtering method was employed to denoise images. Denoised images were subject to binarization processing by histogram threshold segmentation method and between-cluster variance threshold segmentation method, to lay the foundation for subsequent feature extraction of road cracks.

**KEYWORDS;**-Road crack detection, Wiener filter, Cluster variance, Image processing

Date of Submission: 08-05-2020

Date of Acceptance: 22-05-2020

### I. INTRODUCTION

Other than subgrade settlement, pavement cracks are one of the most common road defects and an important factor for major road structures to damage or collapse due to instability [1,2]. Currently, for the road crack detection, crack observation instruments are mostly used to measure data, which will be manually observed and judged [3]. Such method consumes time and labor, is strongly subjective and not favorable for objective evaluation on road structure safety. In recent years, as large-scale wireless multimedia sensor networks (WMSN) technology advances, it is possible to detect road cracks at large using the abundant multimedia nodes of WMSN [4-6].

For road crack images collected via WMSN nodes, the key to distinguish cracks and normal pavement lies in edges. Distinctive edges are basic conditions to judge whether cracks exist, and also important evidences to extract crack information and evaluate crack damage degree. Affected by environment and equipment, crack images collected via WMSN nodes inevitably include many noises. Therefore, proper image filtering and segmentation methods are determined through analysis and comparison, to preserve better edge details of cracks. This is important for further extraction of geometrical characteristics of cracks [7-9].

Image processing methods of road crack detection were studied. Through the analysis and comparison on advantages and disadvantages of average filtering, median filtering, and Wiener filtering, Wiener filtering method was employed to denoise images. Denoised images were subject to binarization processing by histogram threshold segmentation method and between-cluster variance threshold segmentation method, to lay the foundation for subsequent feature extraction of road cracks.

The rest of this paper is organized as follows. In Section 2, we introduced the components of road crack detection system. In Section 3, we explained the principle of road crack image processing methods, including three kinds of image filtering methods and two kinds of image segmentation methods. In Section 4, we discussed the experimental results. And in Section 5 we drawn the conclusions.

### II. THE COMPONENTS OF ROAD CRACK DETECTION SYSTEM

As a novel distributed sensing and monitoring network, WMSN integrates sensor technology, distributed information processing technology, network topology routing protocol, image processing technology, multimedia data transmission, and wireless communication network technology, uses many multimedia sensor nodes as main part, thus being able to sense and monitor regional abundant multimedia information including audios, videos, images, and values and monitor application environments accurately and comprehensively in a fine-grained way, greatly enhancing the monitoring capability of the objective world and environments, presenting very important research value and long-term application prospect [10,11]. The structure of WMSN-based road crack detection system is shown in Fig. 1.

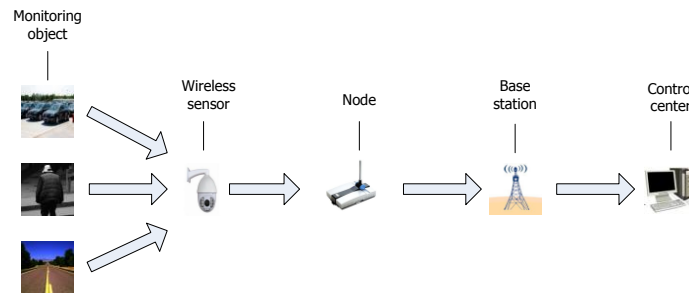


Fig. 1. The bioartificial of road crack detection system

### III. DISCUSSION OF PROCESSING METHODS FOR ROAD CRACK IMAGES

There are many external intrusive factors in road monitoring scenarios. Due to the effects of light scattering in outdoor monitoring environment, images will have changed chroma, lowered contrast ratio, suffer from stripes, flickers and other image quality problems. Moreover, the images collected under conditions of severe weather or illumination variation contain a lot of noises, usually come with low signal-to-noise ratio, narrow dynamic range, small resolution ratio, insufficient contrast ratio among others, thus covering basic features of images, deteriorating visual effects, and greatly affecting the reliability of road monitoring [12-14]. For the issues above, image processing methods of road cracks were compared and discussed in this section, including three common filtering methods and two segmentation methods, to prepare for subsequent work.

#### The principle of road crack image filtering method

In general, a road crack image without displacement change can be expressed by the equation below:

$$f(x, y) = g(x, y) + z(x, y) \quad (1)$$

Where, matrices  $f(x, y)$ ,  $g(x, y)$  and  $z(x, y)$  refer to the noise introduced for observed images, original images, and during degradation process. Image filtering aims to denoise the model above or reduce noise  $z(x, y)$  impact, to minimize the difference between the observed image  $f(x, y)$  and the original image  $g(x, y)$  [15].

Common filtering methods in the image processing field are mean filtering [16], median filtering [17], and Wiener filtering [18], of which the principles are described below separately.

Mean filtering, also neighborhood averaging, falls to low-frequency filtering range. This method allows low-frequency noises of images to pass through the filter and remove high-frequency noises, to achieve the purpose of eliminating high-frequency noises, as shown in Equation (2).

$$h_1(x, y) = \frac{1}{M} f(x, y) \quad (2)$$

In Equation (2),  $h_1(x, y)$  is the image processed by average filtering, while  $f(x, y)$  is the observed image input by filter.

Median filtering is a non-linear image processing method, and is a typical application of order-statistic filter. The difference from the average filtering is that the median filtering decides grayscale of center pixels based on ranking results of intra-neighborhood pixels by grayscale, as shown in Equation (3).

$$h_2(x, y) = \text{median}[f(x_1, y_1), f(x_2, y_2), \dots, f(x_n, y_n)] \quad (3)$$

In Equation (3),  $h_2(x, y)$  is the image processed by average filtering, and the right part of the equal sign means the median of pixel grayscales in the observed image selected.

Wiener filtering assumes that the input of a liner filter is the sum of useful signals and noise, both of which are in wide-sense stationary process and of known second-order statistical characteristics. Parameters of the optimum liner filter are calculated based on the minimum mean square error criterion. The liner filter is an adaptive minimum mean square error filter. As a statistical method, Wiener filtering adopts the optimal criterion based on correlation matrices of images and noise, is able to adjust the output of the filter based on local variance of images. The bigger the local variance of images, the stronger smoothing effects of the filter. It is expressed by Equation (4).

$$h_3(x, y) = \mu + \frac{\sigma^2 - v^2}{\sigma^2} [f(x, y) - \mu] \quad (4)$$

Where  $\mu$ ,  $\sigma^2$  and  $v^2$  refer to average, variance, and noise square error of images, respectively.  $\mu$  and  $\sigma^2$  are expressed by Equation (5) and Equation (6).

$$\mu = \frac{1}{M} \sum_{i=1}^M f(x_i, y_i) \tag{5}$$

$$\sigma^2 = \frac{1}{M} \sum_{i=1}^M \sigma^2(x_i, y_i) - \mu^2 \tag{6}$$

**The theory of road crack image segmentation method**

To better analyze road cracks, road cracks shall be separated from observed images. Basically, crack areas on images have different grayscale from background areas, so cracks and background can be segmented by setting a threshold. Now the threshold segmentation methods which have been successfully transplanted to relevant hardware platforms and widely applied are histogram threshold segmentation method [19] and OTSU threshold segmentation method [20].

Histogram threshold segmentation method is a visual inspection threshold method proposed by Prewitt. Its theory is to describe a grayscale image as  $f(x, y)$  by a 2D matrix. Where  $f$  refers to the pixel grayscale at  $(x, y)$ . If there is a grayscale threshold  $T$  which is able to divide all pixels on images into target and background, then targets can be separated through finding out this threshold  $T$ .

The maximum between-cluster variance threshold segmentation method (OTSU threshold segmentation method) proposed by Japanese scholar OTSU is one of the most widely applied image segmentation methods and adopts the maximum between-cluster variance of images as segmentation threshold criterion. Its theory can be simply explained below.

It is assumed that there is an image with  $M$  pixels, with the grayscale level range of  $[0, L-1]$ .  $a_i$  refers to the number of image pixels with the grayscale level of  $i$ , then the probability of pixels at each grayscale level on a whole image is  $p_i = a_i/M$ . If a single threshold  $T$  can be found, then the image can be divided into the area  $f_1(x, y)$  with the grayscale range of  $[0, T]$  and the area  $f_2(x, y)$  with the grayscale range of  $[T+1, L-1]$ . In this case, the grayscale average of the whole image, region  $f_1(x, y)$  and region  $f_2(x, y)$  can be calculated from Equation (7):

$$\mu_f = \sum_{i=0}^{L-1} ip_i, \quad \mu_{f_1} = \sum_{i=0}^T ip_i / \eta_{f_1}, \quad \mu_{f_2} = \sum_{i=T+1}^{L-1} ip_i / \eta_{f_2} \tag{7}$$

Where,  $\mu_f, \mu_{f_1}, \mu_{f_2}$  refer to grayscale average of the whole image, region  $f_1(x, y)$  and region  $f_2(x, y)$ , while  $\eta_{f_1}, \eta_{f_2}$  refer to probability of pixels in region  $f_1(x, y)$  and region  $f_2(x, y)$  to the whole image. Therefore, the between-cluster variance of the image can be defined as:

$$\sigma_\eta^2 = \eta_{f_1} (\mu_{f_1} - \mu)^2 + \eta_{f_2} (\mu_{f_2} - \mu)^2 \tag{8}$$

When the maximum between-cluster variance is obtained, the optimal segmentation threshold (Otsu threshold) can be expressed by:

$$\hat{T} = \arg \max_{0 \leq T \leq L-1} \sigma_\eta^2 \tag{9}$$

**IV. EXPERIMENTS**

To work out proper filtering methods and threshold segmentation methods for processing images of road cracks, several algorithms mentioned here are experimented comparatively. To ensure the evaluation objectivity, the denoising effects of filtering algorithms can be measured by peak signal to noise ratio (PSNR) and mean square error (MSE), except visual judgment. Bigger PSNR and smaller MSE indicate better filtering results and better retention degree of image features. All the experiments are promoted on a Inter(R) Core(TM) i5 PC with 8 GB RAM.

In the first experiment, we compared the PSNR and MSE results by using mean filtering, median filtering, and wiener filtering. The tests were performed on three crack images, which are given in Fig. 2. Each image has a size of 500×354 pixels, and the bit depth is 8. White noise with variations of 0.1, 0.2, 0.3 and 0.5 were added in the images. The results are given in table 1 to table 3.

By watching the data shown in the above tables, it can be found that the PSNR results obtained by the wiener filtering are better than those of the other methods for the same image. For example, by adding white noise with variance of 0.1 to the crack image 1, the PSNR result obtained by wiener filtering is 15.6373 dB, with the increased value by 0.8415 dB and 9.956 dB respectively compared to the values in mean filtering and median filtering. Meanwhile, we found that Wiener filtering doesn't show the optimum results on MSE, but presents better results than median filtering and slightly worse than average filtering on noise variance.

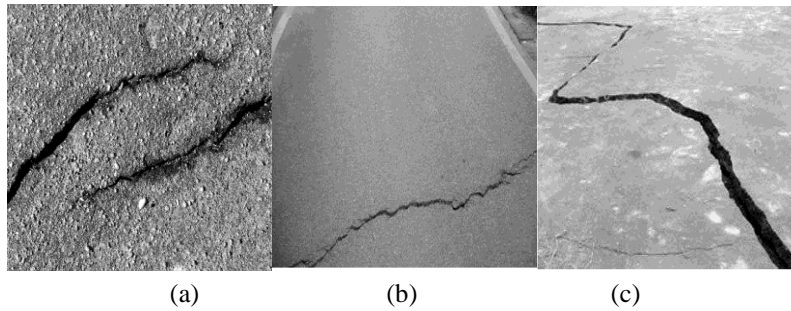


Fig. 2. The original images: Crack Image 1 (a), Crack Image 2 (b), and Crack Image 3 (c).

We also found that the PSNR results obtained by wiener filtering are better than the others for different images. For instance, by adding white noise with variance of 0.5, the PSNR result obtained by wiener filtering is increased by 3.34 dB and 0.44 dB on average, respectively to mean filtering and median filtering.

|        | $v=0.1$ |        | $v=0.2$ |        | $v=0.3$ |        | $v=0.5$ |        |
|--------|---------|--------|---------|--------|---------|--------|---------|--------|
|        | PSNR    | MSE    | PSNR    | MSE    | PSNR    | MSE    | PSNR    | MSE    |
| Mean   | 5.6813  | 1757.7 | 5.6869  | 1755.5 | 5.6920  | 1753.4 | 5.6997  | 1750.3 |
| Median | 14.7958 | 2155.3 | 12.0342 | 4070.6 | 9.5292  | 7247.1 | 6.2267  | 1550.3 |
| Wiener | 15.6373 | 1775.6 | 12.5674 | 3600.3 | 10.0886 | 6371.1 | 7.0291  | 1288.7 |

Table 1. Performance of the filtering methods of crack image 1

|        | $v=0.1$ |        | $v=0.2$ |        | $v=0.3$ |        | $v=0.5$ |        |
|--------|---------|--------|---------|--------|---------|--------|---------|--------|
|        | PSNR    | MSE    | PSNR    | MSE    | PSNR    | MSE    | PSNR    | MSE    |
| Mean   | 5.3051  | 1916.8 | 5.3111  | 1914.1 | 5.3169  | 1911.6 | 5.3248  | 1908.1 |
| Median | 19.2855 | 766.5  | 13.8328 | 2690.3 | 10.4406 | 5875.2 | 6.9285  | 1319.0 |
| Wiener | 19.4212 | 742.9  | 13.9007 | 2648.6 | 10.5828 | 5685.9 | 7.3059  | 1209.2 |

Table 2. Performance of the denoising methods of crack image 2

|        | $v=0.1$ |        | $v=0.2$ |        | $v=0.3$ |        | $v=0.5$ |        |
|--------|---------|--------|---------|--------|---------|--------|---------|--------|
|        | PSNR    | MSE    | PSNR    | MSE    | PSNR    | MSE    | PSNR    | MSE    |
| Mean   | 3.2649  | 3066.1 | 3.2691  | 3063.2 | 3.2722  | 3061.0 | 3.2743  | 3059.5 |
| Median | 19.0348 | 812.1  | 13.8638 | 2671.2 | 11.0671 | 5086.0 | 9.8575  | 6719.3 |
| Wiener | 19.6382 | 706.7  | 14.4467 | 2335.7 | 11.8006 | 4295.6 | 9.9839  | 6526.7 |

Table 3. Performance of the denoising methods of crack image 3

In the second experiment, three test images were added with Gaussian noise with the variance  $v$  of 0.5 and subject to comparative filtering experiment. The results are shown in Fig. 3. Based on these results, images processed by average filtering and median filtering are fuzzy, present less obvious edges of road cracks and certain ringing effects. Visual results by Wiener filtering are much better, which can denoise and preserve better image edge features.

As a final experiment, three test images were subject to threshold segmentation experiment by histogram threshold segmentation method and OTSU threshold segmentation method. The results are shown in Fig. 4. Seen from Fig. 4, we found that, through binarization processing by histogram threshold segmentation method, good results are obtained for test image 1 while poor results for test image 2 and test image 3, causing that characteristics are almost lost completely and cannot be used for next processing. Through binarization processing by OTSU threshold segmentation method, good results are obtained for test image 1 and test image 3, presenting road cracks clearly and preserving complete edge details. Though the results for test image 2 by OTSU method are worse than the other two images, road cracks can be observed and are better than the results by histogram threshold segmentation method. This is because in test image 2, there are two road markings apart from the existence of cracks with different grayscale from pavement background, so that the peak and valley on grayscale histogram of the image are not distributed theoretically, leading to poor threshold segmentation results.

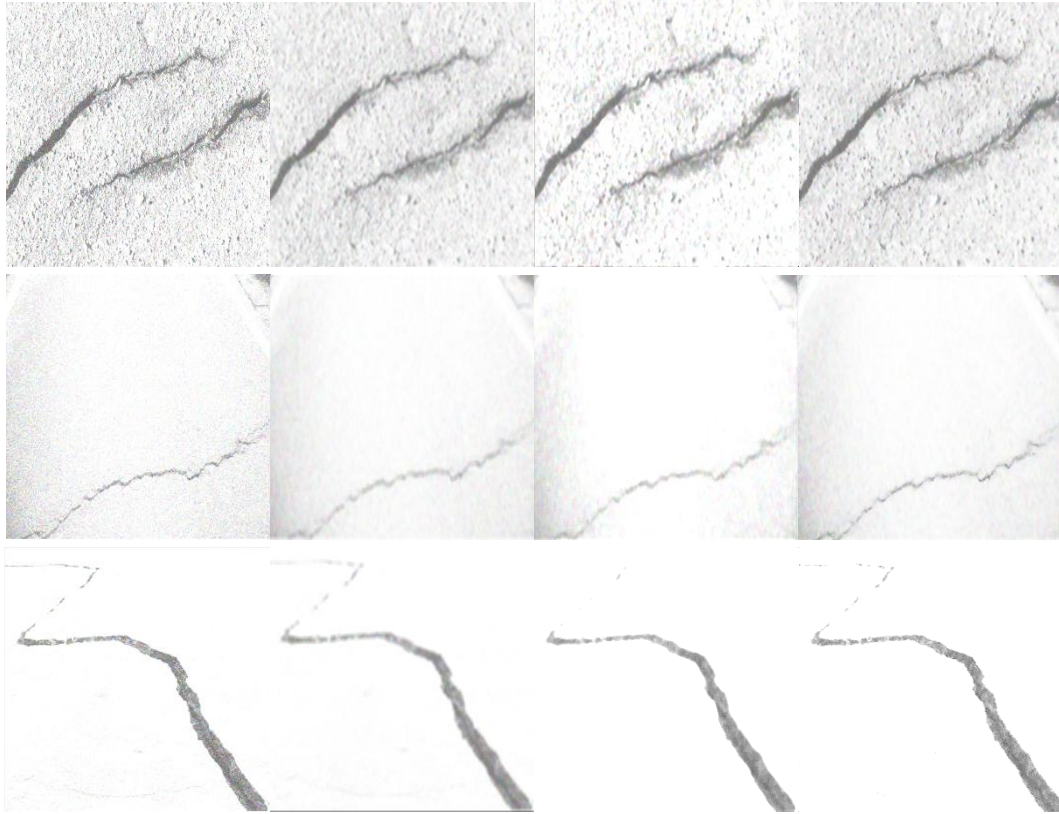


**Fig. 3. Visual comparison of the filtering results on three crack images, from top to bottom are crack image 1, crack image 2, and crack image 3 ( $v = 0.5$ ). The first column: noisy image, the second column: mean, the third column: Median, the final column: Wiener.**

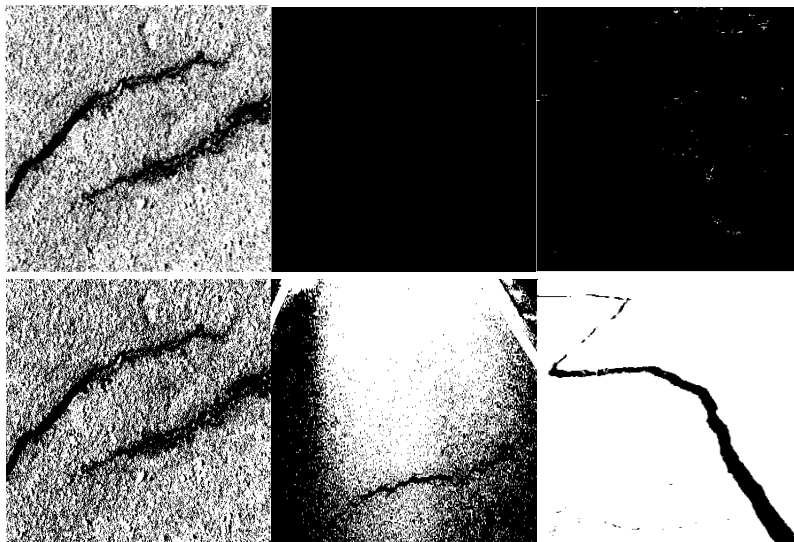


**Fig. 4. Visual comparison for two kinds of segmentation methods on three crack images, from left to right are results on crack image 1 (a), results on crack image 2 (b), and results on crack image 3 (c), respectively.**

## V. CONCLUSION

In this paper, image processing methods of road crack detection were studied; the collection possibility of crack images by WMSN system were discussed; the image enhancement method based on average filtering, median filtering, and Wiener filtering as well as the image binarization segmentation method based on histogram threshold segmentation method and OTSU threshold segmentation method were analyzed. Experimental results show that Wiener filtering can effectively filter and remove Gaussian noise on images,

while OTSU method can properly distinguish between image target and background, and preserve target edges and other details. The research results lay the foundation for the next extraction of crack characteristics.

#### ACKNOWLEDGMENTS

This paper is supported by the Scientific Research Fund of Hunan Provincial Education Department under Grant No 19B105, and Yiyang Science and Technology Bureau under Grants number YKZ [2016] 51 & 2017YC01. The authors would like to thank the anonymous reviewers for their insightful comments and suggestions, which have greatly improved this paper.

#### REFERENCE

- [1]. Seongdeok Bang, Somin Park, Hongjo Kim, Hyoungkwan Kim, "Encoder-decoder network for pixel-level road crack detection in black-box images", *Computer-Aided Civil and Infrastructure Engineering*, (34): 713-727, 2019.
- [2]. Somin Park, Seongdeok Bang, Hongjo Kim, Hyoungkwan Kim, "Patch-Based Crack Detection in Black Box Images Using Convolutional Neural Networks", *Journal of Computing in Civil Engineering*, (33): 1-10, 2019.
- [3]. Jun Jo, Zahra Jadidi, "A high precision crack classification system using multi-layered image processing and deep belief learning" *Structure and Infrastructure Engineering*, 16(2): 297-305, 2020.
- [4]. M. Nava, Barathy, Deje, "Two-level data aggregation for WMSNs employing a novel VBEO and HOSVD", *Computer Communications*, (149): 194-213, 2020.
- [5]. Ala-Eddine Benrazek, Brahim Farou, Hamid Seridi, Zineddine Kouahla, Muhammet Kurulay, "Ascending hierarchical classification for camera clustering based on FoV overlaps for WMSN", *IET Wireless Sensor Systems*, 9(6): 382-388, 2019.
- [6]. Feng Wenzhao, Hu Chunhe, Wang Yuan, Zhang Junguo, Yan Hao, "A Novel Hierarchical Coding Progressive Transmission Method for WMSN Wildlife Images", *Sensors*, 19(4): 946, 2019.
- [7]. Yang Yang, Songtao Guo, Guiyan Liu, Yuanyuan Yang, "Two-layer compressive sensing based video encoding and decoding framework for WMSN", *Journal of Network and Computer Applications*, (117): 72-85, 2018.
- [8]. Jeehyeong Kim, Teasung Kim, Jaewon Noh, Sunghyun Cho, "Fractional Frequency Reuse Scheme for Device to Device Communication Underlying Cellular on Wireless Multimedia Sensor Networks", *Sensors*, 18(8): 2661, 2018.
- [9]. Fan He, Haiping Huang, Ruchuan Wang, Lingyun Jiang, "Data fusion-oriented cluster routing protocol for multimedia sensor networks based on the degree of image difference", *CCF Transactions on Networking*, 1: 65-77, 2019.
- [10]. Ru Jingyu, Jia Zixi, Yang Yufang, Yu Xiaosheng, Wu Chengdong, Xu Ming, "A 3D Coverage Algorithm Based on Complex Surfaces for UAVs in Wireless Multimedia Sensor Networks", *Sensors*, 19(8): 1902, 2019.
- [11]. Addisalem Genta, D. K. Lobiyal, Jemal H. Abawajy, "Energy Efficient Multipath Routing Algorithm for Wireless Multimedia Sensor Network", *Sensors*, 19(17): 3642, 2019.
- [12]. Sara Khalid, Nazeer Muhammad, Muhammad Sharif, "Automatic measurement of the traffic sign with digital segmentation and recognition", *IET Intelligent Transport Systems*, 13(2): 269, 2018.
- [13]. Teresa Pamula, "Road Traffic Conditions Classification Based on Multilevel Filtering of Image Content Using Convolutional Neural Networks", *IEEE Intelligent Transportation Systems Magazine*, 10(3): 11-21, 2018.
- [14]. Dilbag Singh, Vijay Kumar, "Defogging of road images using gain coefficient-based trilateral filter", *International Society for Optics and Photonics*, 1: 013004, 2017.
- [15]. K. Madhan Kumar, A. Velayudham, R. Kanthavel, "An Efficient Method for Road Tracking from Satellite Images Using Hybrid Multi-Kernel Partial Least Square Analysis and Particle Filter", *Journal of Circuits, Systems and Computers*, 26(11): 1750181, 2017.
- [16]. Navdeep Goel, Harpreet Kaur, Jyoti Saxena, "Modified decision based unsymmetric adaptive neighborhood trimmed mean filter for removal of very high density salt and pepper noise", *Multimedia Tools and Applications*, 1-30, 2020.
- [17]. Anwar Shah, Aved Iqbal Bangash, Abdul Waheed Khan, Imran Ahmed, Abdullah Khan, Asfandyar Khan, Arshad Khan, "Comparative analysis of median filter and its variants for removal of impulse noise from gray scale images", *Journal of King Saud University - Computer and Information Sciences*, 4: 1-15, 2020.
- [18]. V. N. Karnaukhov, V. I. Kober, M. G. Mozerov, "Artifact Suppression with Geodesic Kernel Filter for Defocused Images Restored by Wiener Filtering", *Journal of Communications Technology and Electronics*, 64(12): 1458-1463, 2019.
- [19]. P. Mohamed Shakeel, Mohamad Ishak Desa, M. A., "Burhanuddin. Improved watershed histogram thresholding with probabilistic neural networks for lung cancer diagnosis for CBMIR systems", *Multimedia Tools and Applications*, 1-19, 2019.
- [20]. Mohammadi-Sardo Saber, Labibi Fateme, Shafiei Seyed Ali, "A new approach for detecting abnormalities in mammograms using a computer-aided windowing system based on Otsu's method", *Radiological physics and technology*, 12(2): 178-184, 2019.

Zhi Cui, et. al. "Research on Road Crack Detection Based on Image Processing." *The International Journal of Engineering and Science (IJES)*, 9(5), (2020): pp. 16-21.